THE ASTROPHYSICAL JOURNAL, 299:1067–1078, 1985 December 15

EQUILIBRIUM AND NONEQUILIBRIUM CHEMISTRY OF SATURN'S ATMOSPHERE: IMPLICATIONS FOR THE OBSERVABILITY OF PH_3, N_2, CO, AND GeH_4

BRUCE FEGLEY, JR., AND RONALD G. PRINN
Department of Earth, Atmospheric, and Planetary Sciences, Massachusetts Institute of Technology
Received 1985 March 25; accepted 1985 June 13

ABSTRACT

Results are presented for the first comprehensive set of thermochemical equilibrium calculations for several hundred gases in Saturn's hot deep atmosphere. The thermochemical kinetics of the important destruction reactions for the most abundant equilibrium gases are incorporated in a simple chemical-dynamical model to provide predictions of nonequilibrium trace gas abundances in the cool upper atmosphere. A baseline model assuming an adiabatic lapse rate in Saturn's troposphere, 2.5 times solar elemental abundances (except for H_2 and He, where the *Voyager* data are used), and a vertical eddy diffusion coefficient of $K = 2 \times 10^8$ cm^2 s^{-1} was employed; the sensitivity of the results to variations in elemental abundances and K values was studied. The most abundant nonequilibrium trace gas derived from Saturn's deep atmosphere is predicted to be N_2; other important nonequilibrium species include PH_3, CO, GeH_4, HCN, and CH_3NH_2. Only PH_3 has been observed on Saturn. The observation of PH_3 at 1–3 times solar abundance and the observed upper limit for the GeH_4 mixing ratio of 10^{-10} presents an apparent paradox: the predicted GeH_4 mixing ratio consistent with this amount of PH_3 is over 70 times greater than its observed upper limit. This paradox is resolved if we take into account the destruction of GeH_4 by reaction with H atoms from NH_3 and PH_3 photolysis and the photochemical destruction of GeH_4 above the clouds, and the fact that we see well below the uppermost clouds on Jupiter but not on Saturn. While vertical mixing from Saturn's deep atmosphere is predicted to be the major source of N_2, PH_3, HCN, and CH_3NH_2 in Saturn's visible atmosphere, photochemical reactions may effectively compete with vertical mixing as a source of CO.

Subject headings: planets: abundances — planets: atmospheres — planets: Saturn

I. INTRODUCTION

The observations of the disequilibrium species PH_3, CO, and GeH_4 on Jupiter (see, e.g., Beer and Taylor 1978; Fink, Larson, and Treffers 1978; Larson, Treffers, and Fink 1977; Larson, Fink, and Treffers 1978; Ridgway, Larson, and Fink 1976, and references therein) and of PH_3 on Saturn (Larson *et al.* 1980; Courtin *et al.* 1984) can be used to deduce the strength of vertical mixing in the deep atmospheres of these planets (Prinn and Barshay 1977). These deductions are particularly valuable in the study of the atmospheres of Jupiter and Saturn because they refer to regions of their atmospheres which cannot be sampled by entry probes and which are inaccessible to remote sensing techniques.

Extensive thermochemical calculations of the chemistry of Jupiter's atmosphere (Lewis 1969; Barshay and Lewis 1978; Fegley and Lewis 1979) show that the observed PH_3, CO and GeH_4 abundances are many orders of magnitude larger than those predicted at complete thermochemical equilibrium in the cool, visible regions of Jupiter's atmosphere. The observed PH_3, CO, and GeH_4 abundances can, however, be supplied by sufficiently rapid vertical mixing of gas from the hot (800–1300 K) region in Jupiter's deep atmosphere where their abundances are much greater. Such vertical mixing would have to be rapid enough to transport gas parcels upward to cooler regions before thermochemical reactions destroying the unstable molecules could proceed appreciably. In fact, Prinn and Barshay (1977) demonstrated that the observed CO volume mixing ratio of 10^{-9} is compatible with the kinetics of the relevant destruction reactions and with eddy diffusion coefficients (and thus vertical mixing rates) independently estimated from considerations of Jupiter's emitted heat flux (Stone 1976; Flasar and Gierasch 1977).

This (putative) rapid vertical mixing should also be a source of other disequilibrium species which are transported upward before they are destroyed by thermochemical reactions (e.g., oxidation, sulfurization, hydrogenation, etc.). Adopting this philosophy, Barshay and Lewis (1978) and Fegley and Lewis (1979) proposed a number of other potentially observable chemical probes of Jupiter's deep atmosphere including AsH_3, H_2Se, HCl, HF, InBr, TlI, and SbS. Prinn and Olaguer (1981) extended this approach by using kinetic data for homogeneous gas-phase and heterogeneous iron-catalyzed reactions between N_2 and H_2. They predicted that N_2 may be the most abundant chemical probe of the deep atmosphere with a volume mixing ratio of 0.6–10 $\times$ 10^{-6}, depending on whether iron-catalyzed reactions reforming NH_3 are effective in Jupiter's deep atmosphere.

However, despite the now extensive body of spectroscopic data for Saturn, no comprehensive thermochemical-dynamical model is available for the deep atmosphere of this planet. Such a model would have great utility for interpreting existing spectroscopic data, for guiding future observations, and for planning experiments on an entry probe mission.

In this paper we present the results of the first set of comprehensive thermochemical calculations on the chemistry of several hundred gases in Saturn's atmosphere. Kinetic calculations for selected gas-phase and heterogeneous reactions are also presented. The results of these calculations are then used for several purposes: (*a*) interpreting the abundance of the observed PH_3 in terms of vertical mixing from specific atmospheric levels, (*b*) predicting other potentially observable

chemical probes of Saturn's deep atmosphere, (*c*) placing upper limits on gas abundances from deep atmospheric sources, (*d*) contrasting the inferred chemistry and dynamics of the deep atmospheres of Jupiter and Saturn, and (*e*) evaluating models for the origin and composition of Saturn.

II. THERMOCHEMICAL MODEL OF SATURN'S ATMOSPHERE

A variety of evidence (e.g., infrared, microwave, and radio-wavelength observations) indicates that Saturn, like Jupiter, has a deep convective atmosphere. Compositional models also indicate that Saturn's deep atmosphere is convective (see Hubbard and Stevenson 1984, and references therein). Assuming that the temperature gradient in the atmosphere beneath the tropopause is adiabatic, and taking $T_0 = 136$ K at $P_0 = 1$ bar (Prinn *et al.* 1984), the temperature-pressure profile in Saturn's deep atmosphere was calculated stepwise using the relationship

$$\log_{10}(P_{n+1}/P_n) = \mathrm{Cp}/R \log_{10}(T_{n+1}/T_n), \quad (1)$$

where Cp is the temperature-dependent heat capacity of atmospheric gas, $n = 0, 1, 2$, etc., and R is the universal gas constant. The atmospheric composition must be known before equation (1) can be used.

Prinn *et al.* (1984) critically reviewed the available Earth-based, Earth-orbital, and *Voyager* spectroscopic observations of Saturn's atmosphere. This summary shows that while Saturn's atmosphere has approximately solar composition, it is apparently slightly depleted in He and is enriched in ice- and rock-forming elements relative to their solar composition values as defined by Cameron (1982). Based on this critical review, we have adopted a chemical model for Saturn's atmosphere with H_2 and He volume mixing ratios of 0.932 and 0.068 respectively. The carbon mixing ratio is set equal to the observed CH_4 mixing ratio, which is about 2.5 times the solar value, and the mixing ratios of all other elements are also set equal to 2.5 times their solar composition values. (The effects of selected variations in these mixing ratios has also been investigated and will be discussed later). This chemical model was also used to calculate a depth scale for the calculated Saturn adiabat assuming hydrostatic equilibrium. Thus, in finite difference form,

$$Z_{n+1} - Z_n = \mathrm{Cp}(T_{n+1} - T_n)/(\mu g), \quad (2)$$

where Z is depth, μ is the molecular weight of the atmospheric gas (2.15 g mole^{-1}), and g is the mean gravitational acceleration over the entire planet (1117 cm s^{-2}). The starting point is $T_0 = 136$ K, $Z_0 = 0$ km.

The chemical elements which are included in our calculations were chosen on the basis of their solar abundance and volatility. Detailed calculations of thermochemical equilibrium were done for the elements H, O, C, N, S, Fe, P, F, Ge, and Se. Scaling of the calculations presented by Lewis (1969), Barshay and Lewis (1978), and Fegley and Lewis (1979) for Jupiter were done for many other elements which are less interesting because of lower abundances or lower volatilities or both. Thus, for example, it is quite easy to show that if Mg, Si, Na, and K are totally condensed out of the Jovian atmosphere at levels hundreds of kilometers beneath the visible cloud tops, then the same situation will prevail on Saturn. Analogously, volatile but extremely minor constituents of the Jovian atmosphere such as Hg, InBr, and TlI will also be present on Saturn at abundances which are easily calculated by scaling (see, e.g., calculations in § 4.1 of Prinn *et al.* 1984). In this fashion a total of 44 elements and approximately 700 compounds (see Appendices to Barshay and Lewis 1978 and Fegley and Lewis 1979) has been considered.

The thermochemical equilibrium calculations were done by simultaneously considering the constraints of mass balance and chemical equilibrium. Calculations were done at temperatures ranging from 300 to 3000 K along the calculated Saturn adiabat. A detailed description of the general method used is given by Barshay and Lewis (1978). Thermodynamic data were taken from several standard sources, such as the JANAF Tables (Stull and Prophet 1971–1985); Kelley (1960); Kelley and King (1961); Stull, Westrum, and Sinke (1969); Wagman *et al.* (1968); and Glushko *et al.* (1978–1982). The results of these calculations are summarized in Figures 1–4, in which volume mixing ratios of various gases along the Saturn adiabat are plotted as a function of inverse temperature. In order to simplify the graphical representations, not all the gases included in the calculations are plotted. However, the most abundant gases for each element are always plotted, and the gases not illustrated are generally $\leq 10^{-6}$ of the abundance of that element.

III. RESULTS OF THERMOCHEMICAL EQUILIBRIUM CALCULATIONS

The calculated equilibrium mixing ratios of the most abundant carbon-bearing gases are illustrated in Figures 1 and 2. Methane is the most abundant carbon-bearing gas at all temperatures less than 3000 K. The free radical CH_3 is the second most abundant gas at $T > 2060$ K, CO is the second most abundant gas at $2060 > T > 1100$ K, and C_2H_6 is the second most abundant gas at $T < 1100$ K. No other carbonaceous gases have mixing ratios greater than 10^{-10} at temperatures of 1000 K or lower.

Both C_2H_2 and C_2H_6 have been observed in Saturn's atmosphere and have mixing ratios of 8×10^{-8} and 4×10^{-6} respectively at pressures less than 20 mbar (Prinn *et al.* 1984). As Prinn *et al.* (1984) further point out, the C_2H_2 and C_2H_6 mixing ratios and their rapid decrease at higher pressures are compatible with photochemical sources for these gases. Our calculations show that comparable mixing ratios for C_2H_2 and C_2H_6 in thermochemical equilibrium with atmospheric gases are not reached until temperatures greater than 3000 K, over 3000 km beneath the visible cloud tops. Thus, a major deep atmospheric contribution to the observed abundances of C_2H_2 and C_2H_6 is not expected. Finally, hydrocarbons with three or more carbon atoms, and other organic compounds (e.g., acids, alcohols, aldehydes, esters, ketones, etc.) with two or more carbon atoms have negligible mixing ratios in thermochemical equilibrium at any temperature.

The calculated equilibrium abundances of the important hydrogen, oxygen, nitrogen, sulfur, and fluorine compounds are also given in Figures 1 and 2. While H_2, H_2O, NH_3, H_2S, and HF are the predicted major gases of H, O, N, S, and F respectively, only H_2 and NH_3 have been observed on Saturn. The absence of H_2O and H_2S in Saturn's upper atmosphere can be plausibly explained by condensation to form clouds of aqueous NH_3, water ice, and NH_4SH (Weidenschilling and Lewis 1973; Prinn *et al.* 1984; Atreya and Romani 1985). Larson *et al.* (1980) point out that their upper limit to Saturn's water abundance (<2 cm amagat) is consistent with the H_2O saturated vapor pressure at the assumed temperature (175 K) of the 5 μm line-forming region (Fink and Larson 1978). Prinn *et al.* (1984) note that as a result of condensation the H_2S

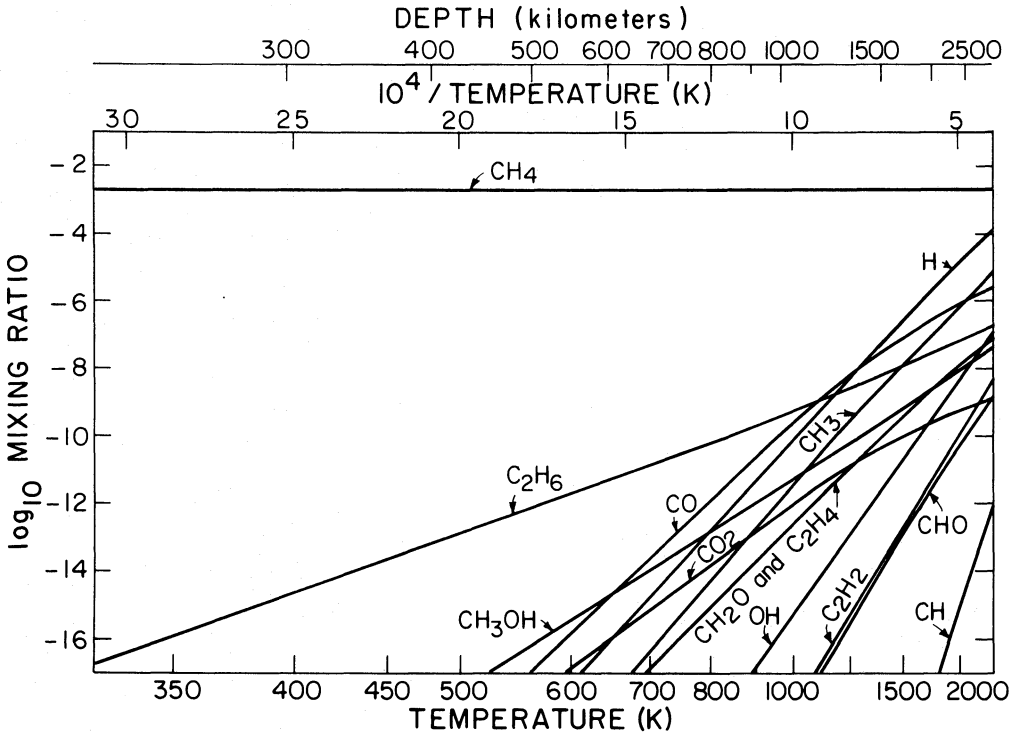

FIG. 1.—Equilibrium abundances of some carbon-containing gases along the model adiabatic (P, T)-profile in Saturn's atmosphere. The horizontal scales indicate temperature and depth along the Saturnian adiabat.

mixing ratio decreases very rapidly above the NH_4SH cloud base (224 K, 4.7 bars for 2.5 times solar N and S abundances) with a scale height $h \approx 3$ km. Solar UV photolysis would reduce the H_2S abundance in Saturn's upper atmosphere even further. Finally, HF is removed by condensation at 330 K to form NH_4F(s), which will probably dissolve in the predicted aqueous NH_3 clouds.

N_2 is the second most abundant nitrogen-bearing gas at all temperatures less than 3000 K and is potentially the most abundant nonequilibrium species in the upper atmosphere (Prinn and Olaguer 1981). The thermochemical kinetics of N_2 formation and destruction reactions and the relative contributions of thermochemical and photochemical (Atreya, Kuhn, and Donahue 1980) N_2 sources will be considered later. All other N species which could potentially be mixed up to visible levels have very low abundances. The deep atmospheric

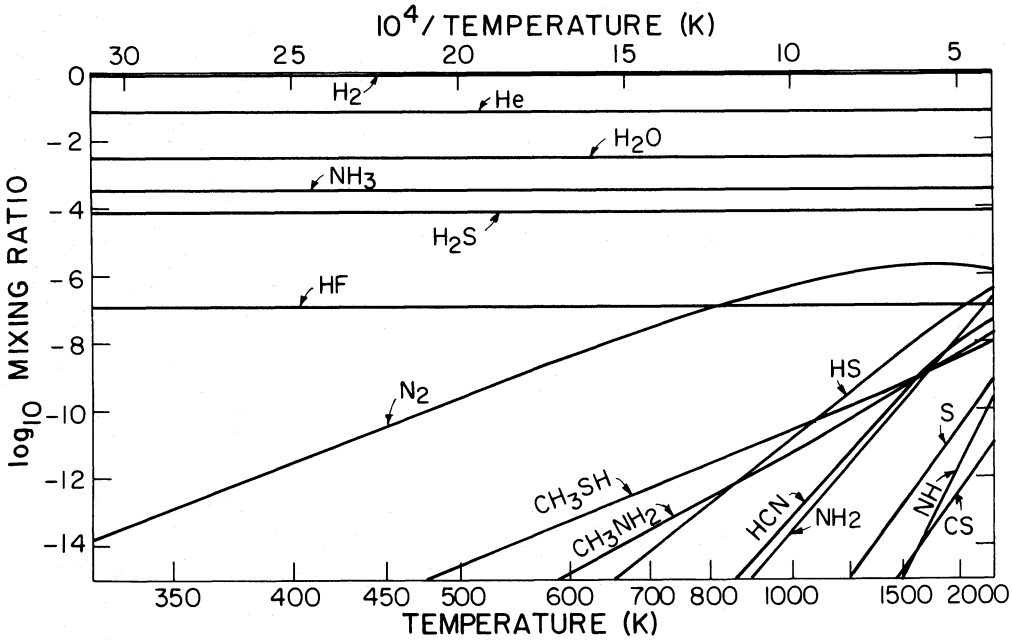

FIG. 2.—As in Fig. 1 but for H_2, He, and oxygen-, nitrogen-, and sulfur-containing gases

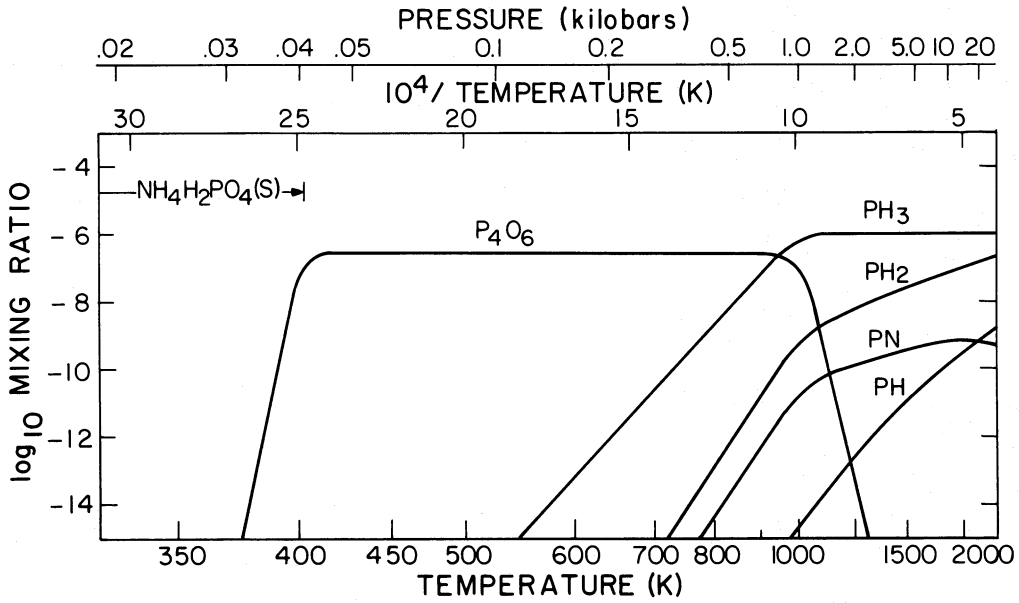

FIG. 3.—As in Fig. 1 but for phosphorus-containing gases. The horizontal scale indicates pressure along the Saturnian adiabat. Condensation of $NH_4H_2PO_4$(s) at 404 K decreases the abundance of P_4O_6(g).

sources for some of these gases (e.g., for HCN and CH_3NH_2) may be comparable nevertheless to the predicted photochemical sources (Kaye and Strobel 1984) and are therefore of interest. For example, Lewis and Fegley (1984) suggested that rapid vertical mixing provides the dominant contribution to tropospheric HCN and CH_3NH_2 on Jupiter.

The calculated equilibrium abundances of phosphorus compounds are shown in Figure 3. It is immediately apparent that if complete thermochemical equilibrium is attained, then the abundance of PH_3 in the visible atmosphere will be negligible. However, the observations reviewed by Prinn *et al.* (1984) show PH_3 mixing ratios of $0.2–2 \times 10^{-6}$, which are 32–33 orders of magnitude larger than the PH_3 mixing ratio predicted assuming thermochemical equilibrium in the visible atmosphere. The PH_3 observations are direct evidence for the existence of a potent disequilibrating mechanism such as rapid vertical mixing.

Sufficiently vigorous vertical mixing should also have a noticeable effect on the GeH_4 abundance. Figure 4 displays the calculated equilibrium abundances of Ge- and Se-bearing gases. Prinn *et al.* (1984) note that the observed GeH_4 mixing ratio on Jupiter of $\sim 7 \times 10^{-10}$ (Kunde *et al.* 1982; Fink, Larson, and Treffers 1978) could be supplied by vertical mixing from the 800 K level (Fegley and Lewis 1979). Taking this temperature as the quench level for thermochemical reactions destroying GeH_4 leads to the prediction that rapid vertical mixing on Saturn should supply a GeH_4 abundance equivalent to a mixing ratio of 6×10^{-9} (see Fig. 4) in the visible atmosphere. However, GeH_4 has not been observed in Saturn's atmosphere, and the upper limit of 10^{-10} for the GeH_4 mixing ratio determined by Larson *et al.* (1980) is 60 times smaller than the abundance predicted by this simple analogy with Jupiter. This apparent discrepancy suggests that significant differences may exist between the vertical mixing rates or the

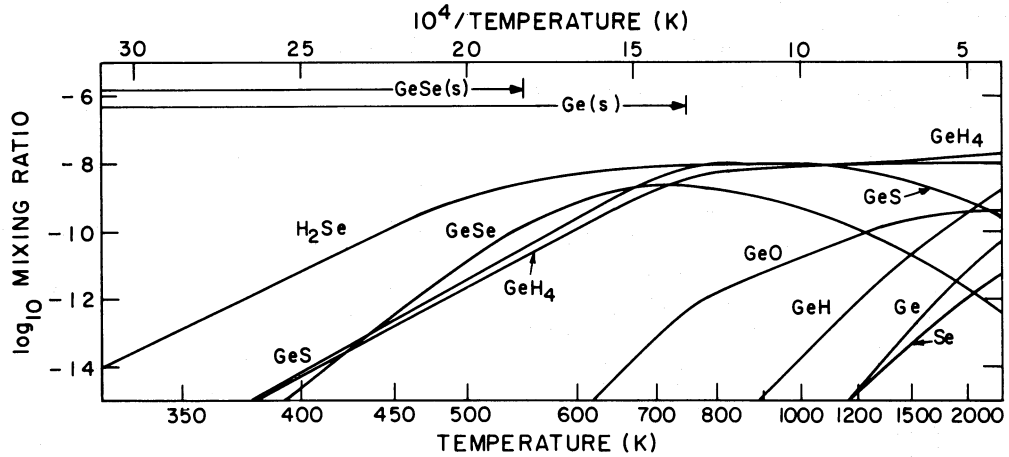

FIG. 4.—As in Fig. 1 but for germanium- and selenium-containing gases. Ge(s) and GeSe(s) condense at 746 K and 546 K respectively. The horizontal lines indicate the temperatures over which the condensates are stable, but not condensate abundances, which can be estimated by the decrease in abundance of the gaseous compounds.

chemistry in the deep atmospheres of Jupiter and Saturn. In order to explore this possibility, we must examine the thermochemical kinetics of the reactions involved in the formation and destruction of PH_3, N_2,CO, and GeH_4.

IV. KINETICS OF THERMOCHEMICAL REACTIONS IN SATURN'S DEEP ATMOSPHERE

The attainment of thermochemical equilibrium for a gas requires that the time constant t_{chem} for the fastest reactions producing and destroying it is much shorter than the time constant t_{conv} for transporting the gas to a cooler region of the atmosphere where these reactions will be kinetically inhibited. Typically, t_{chem} increases more rapidly with increasing altitude (i.e., decreasing temperature) than t_{conv}. Prinn and Barshay (1977) define the altitude $Z = Z^*$ at which $t_{chem} = t_{conv}$ as the quench level for the gas. At lower levels in the atmosphere $Z < Z^*$, $t_{chem} < t_{conv}$ holds, and thermochemical equilibrium is reached. Conversely, at higher altitudes in the atmosphere $Z > Z^*$, $t_{chem} > t_{conv}$ holds, and there is insufficient time to reach thermochemical equilibrium. For reactions with sufficiently large activation energies, once $t_{chem} \approx t_{conv}$, vertical mixing over a very small altitude increment compared to the atmospheric density scale height H results in thermochemical reactions being quenched at the equilibrium concentrations prevailing at level Z^*.

The quench level Z^* differs for each species considered. We derive Z^* by identifying the level where $t_{chem} = t_{conv} \approx H^2/K$, where K is the vertical eddy diffusion coefficient. The quantity K is taken as 2×10^8 cm^2 s^{-1} in our baseline model. This value is consistent with K values of 10^7–10^9 cm^2 s^{-1}, estimated for Saturn's deep atmosphere using the theory for free convection and a knowledge of Saturn's internal heat flux (Prinn *et al.* 1984). Note that this K value refers to the region 1000–2000 km below the visible clouds. Values of K for the visible part of the atmosphere are different and are discussed later. Alternatively, we can define Z^* as the level at which the equilibrium mixing ratio of the species equals its "quenched" mixing ratio, as observed in the visible atmosphere, and proceed to estimate K from the formula

$$K = H^2/t_{chem}(Z^*) . \quad (3)$$

Here we are interested in particular in the thermochemical kinetics of the gases PH_3, CO, GeH_4, and N_2. Prinn and Barshay (1977) and Prinn and Olaguer (1981) assumed that the rate-determining reactions for the gas-phase conversion of CO to CH_4 and of N_2 to NH_3 are

$$CO + H_2 = CH_2O , \quad (4)$$

$$CH_2O + H_2 \rightarrow CH_3 + OH , \quad (5)$$

$$N_2 + H_2 \rightarrow NH + NH . \quad (6)$$

The corresponding equations for the CO and N_2 chemical lifetimes are

$$t_{chem}(CO) \approx [CO]/k_5[H_2][CH_2O] \approx 1/K_4 k_5[H_2]^2 , \quad (7)$$

$$t_{chem}(N_2) \approx 1/k_6[H_2] , \quad (8)$$

where the square brackets denote the number concentrations of the particular molecules, K_4 is the equilibrium constant for reaction (4), and k_5 and k_6 are the rate constants for reactions (5) and (6) given by the equations

$$k_5 \approx 2.3 \times 10^{-10} \exp(-36{,}200/T) \text{ cm}^3 \text{ s}^{-1} , \quad (9)$$

$$k_6 \approx 8.45 \times 10^{-8} \exp(-81{,}515/T) \text{ cm}^3 \text{ s}^{-1} . \quad (10)$$

The relevant number concentrations used in equations (7) and (8) are taken from the results of the thermochemical equilibrium calculations and our atmospheric model. We emphasize that there may exist more rapid (but as yet unidentified) gas-phase destruction reactions for CO and N_2 than (4) and (5). To place an upper limit on their destruction rates we also consider the case when reactions (4), (5), and (6) are catalyzed by metallic iron particles.

Heterogeneous iron-catalyzed reactions for $N_2 + H_2$ were considered using the computational method described by Prinn and Olaguer (1981). Calculations were done for iron particles with radii of 1, 2, 4, and 6 μm; coalescence and sedimentation limit the upward transport of larger particles, and coagulation constrains the population of smaller particles. Figure 5 shows that the predicted N_2 mixing ratio for heterogeneous catalysis increases with decreasing K. If we increase t_{conv} (i.e., decrease the vertical eddy diffusion coefficient K), we also increase t_{chem} because less vigorous vertical mixing results in lower densities of the metallic iron catalyst in the relevant portion of the atmosphere. The points where $K = wH$ (the product of the Stokes sedimentation velocity w and the atmospheric density scale height H) for each particle radius are marked with arrows in Figure 5.

We are unaware of any relevant experimental data for heterogeneous iron-catalyzed reactions converting CO to CH_4. Therefore, heterogeneous catalysis of CO destruction was modeled by using the same t_{chem} values (for a given particle radius and K value) calculated for the $N_2 + H_2$ reactions. Because the presence of iron metal "clouds" on Saturn is only hypothetical (the iron may be sequestered in the core), and because the efficiency of iron catalysis may be reduced by various surface coatings on iron particles (e.g., FeS and Fe_3P), we regard the catalyzed N_2 and CO abundance profiles as firm lower limits. (Note also that the calculated base of the iron metal "cloud" on Saturn is at 4700 K and 560 kbar and our ability to accurately model cloud physics in such conditions is open to question).

The rate-determining reaction and the corresponding rate constant and chemical time constant for destruction of HCN are taken from Prinn and Fegley (1981):

$$HCN + H_2 \rightarrow CH_2 + NH , \quad (11)$$

$$t_{chem}(HCN) \approx 1/k_{11}[H_2] , \quad (12)$$

$$k_{11} = 1.08 \times 10^{-8} \exp(-70{,}456/T) \text{ cm}^3 \text{ s}^{-1} . \quad (13)$$

The thermochemical destruction of PH_3 proceeds via the overall reaction

$$4PH_3 + 6H_2O \rightarrow P_4O_6 + 12H_2 . \quad (14)$$

Prinn *et al.* (1984) suggested one possible mechanism for this reaction in the gas phase

$$PH_3 = PH + H_2 , \quad (15)$$

$$H_2O = OH + H , \quad (16)$$

$$H_2 = H + H , \quad (17)$$

$$PH + OH \rightarrow PO + H_2 , \quad (18)$$

$$PO + OH \rightarrow PO_2 + H , \quad (19)$$

$$2PO + 2PO_2 + 2M \rightarrow P_4O_6 + 2M , \quad (20)$$

where M is another atom or molecule and reaction (18) is the rate-determining step. The chemical lifetime of PH_3 is there-

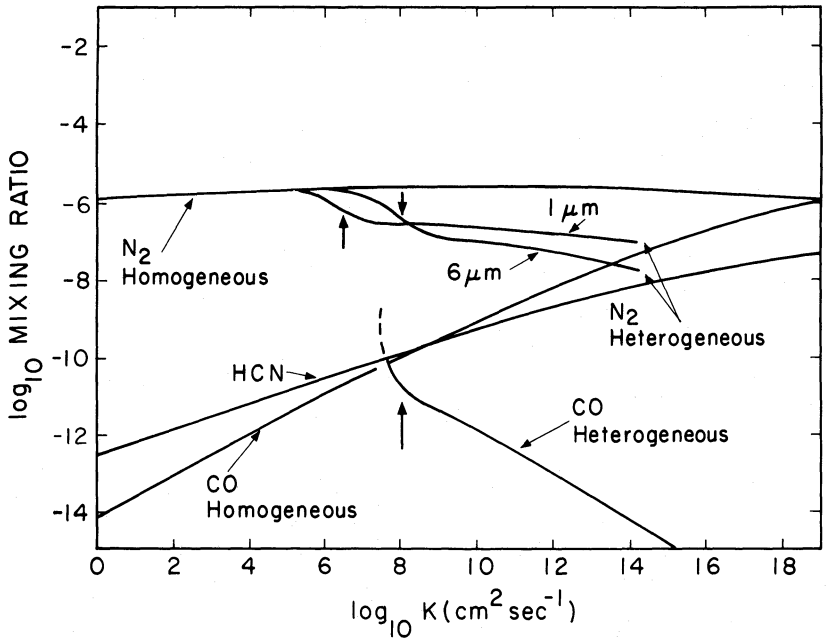

FIG. 5.—Predicted N_2, CO, and HCN mixing ratios in the observable Saturnian atmosphere as a function of the vertical eddy diffusion coefficient K. Homogeneous gas-phase and heterogeneous iron-catalyzed reactions are considered for N_2 and CO. Curves for iron particles with radii of 6 μm (CO) and 1 μm and 6 μm (N_2) are shown. Arrows on these three curves show the point where $K = wH$ (see text). The dashed portion of the CO heterogeneous curve indicates the predicted trend in the *absence* of homogeneous gas-phase reactions. Actual CO mixing ratios at $K < 5 \times 10^7$ cm^2 s^{-1} will follow the homogeneous curve.

fore given by

$$t_{chem}(PH_3) \approx [PH_3]/(k_{18}[PH][OH]) = (K_{17}[H_2]^3)^{1/2}/(k_{18} K_{15} K_{16}[H_2O]) , \quad (21)$$

where the K's are known equilibrium constants and we estimate the rate constant $k_{18} \approx 10^{-9}$ cm^3 s^{-1} at temperatures above 1000 K.

The thermochemical destruction of GeH_4 principally proceeds by the net reaction

$$GeH_4 + H_2S \rightarrow GeS + 3H_2 , \quad (22)$$

although an analogous reaction

$$GeH_4 + H_2Se \rightarrow GeSe + 3H_2 \quad (23)$$

is also important (see Fig. 4). We propose a simple mechanism for reaction (22),

$$GeH_4 = GeH + H_2 + H , \quad (24)$$

$$H_2S = H + SH , \quad (25)$$

$$GeH + SH \rightarrow GeS + H_2 , \quad (26)$$

where reaction (26) is the rate-determining step. In this case the chemical lifetime of GeH_4 is given by

$$t_{chem}(GeH_4) \approx [GeH_4]/(k_{26}[GeH][SH]) = K_{17}[H_2]^2/(k_{26} K_{24} K_{25}[H_2S]) , \quad (27)$$

with k_{26} also estimated as 10^{-9} cm^3 s^{-1} at temperatures above 1000 K. The proposed mechanisms for the conversion of PH_3 to P_4O_6 and of GeH_4 to GeS are difficult to evaluate in the absence of laboratory data on the kinetics of reactions (14) and (22). However, we can use the estimated expressions for the PH_3 and GeH_4 chemical lifetimes and our baseline chemical-dynamical model to predict their expected abundances on Jupiter, where both gases have been observed. The predicted PH_3 and GeH_4 mixing ratios are 5×10^{-7} and 6×10^{-10} (see Fig. 6). The observed PH_3 and GeH_4 mixing ratios are $6 \pm 2 \times 10^{-7}$ and $7 \pm 2 \times 10^{-10}$ (Larson, Fink, and Treffers 1978; Kunde *et al.* 1982). The agreement between the predicted and observed values indicates that our treatment of these two gases is a reasonable first approximation.

V. RESULTS

The results of our chemical-dynamical model for Saturn are presented in Table 1. The predicted PH_3 mixing ratio is identical to that observed by Hanel *et al.* (1981) and very close to that (0.9×10^{-6}) observed by Larson *et al.* (1980). However, the predicted GeH_4 mixing ratio of 7×10^{-9} is about 70 times larger than the upper limit given by Larson *et al.* (1980). Our calculations also predict a CO mixing ratio of 0.07–1.3×10^{-10} and an N_2 mixing ratio of 0.2–2×10^{-6}, depending on whether iron-catalyzed heterogeneous reactions are effective (see Fig. 5). Neither CO nor N_2 has yet been observed on Saturn, but the levels predicted here are undoubtedly beyond current capabilities of remote sensing, particularly given the infrared inactivity of N_2.

The apparent discrepancy between the predicted and observed GeH_4 abundances could be due to several possible effects. Uncertainty in the estimated rate constant for reaction (26) could lead to an overestimate of the amount of GeH_4 transported into Saturn's upper atmosphere by rapid vertical mixing. Alternatively, our neglect of GeH_4 loss by conversion to GeSe could also lead to an overestimate of the GeH_4 abundance. Heterogeneous catalysis of GeH_4 destruction by different types of cloud particles, which would again lead to lower GeH_4 abundances, is also a possible explanation. However, the calculated GeH_4 abundances are relatively insensitive to the

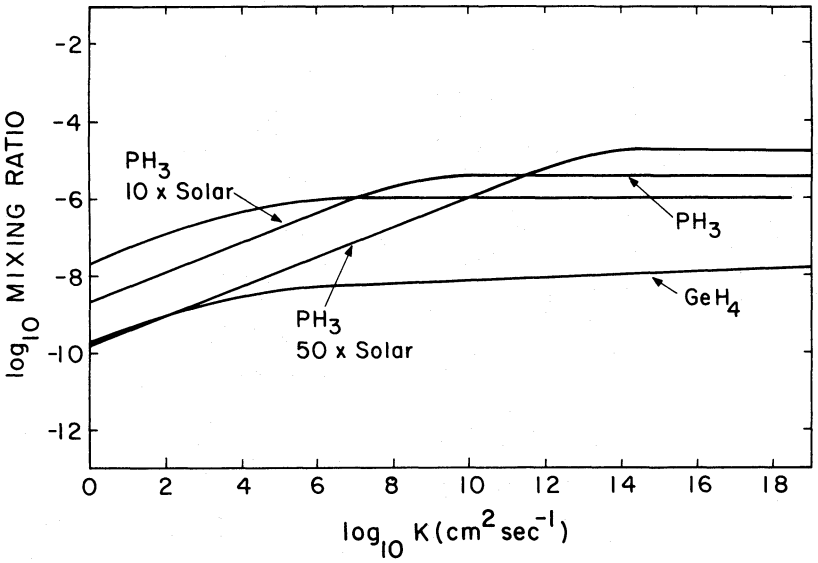

FIG. 6.—As in Fig. 5 for PH_3 and GeH_4. Curves for 2.5 times, 10 times, and 50 times solar elemental abundances are shown for PH_3. The GeH_4 curve is essentially the same at these enrichments.

exact value of k_{26}; varying k_{26} from 10^{-7} to 10^{-11} cm^3 s^{-1} changes the calculated GeH_4 abundances by only a factor of 1.6. Also, GeSe is a minor species relative to GeS over most of the temperature range where thermochemical reactions are expected to be rapid. The two gases do not have equal abundances until below 670 K, by which level Ge(s) condensation is the major GeH_4 loss mechanism. Finally, the good agreement between the predicted and observed GeH_4 abundances on Jupiter suggests that heterogeneous catalysis of GeH_4 destruction is not significant on that planet nor, by inference, on Saturn. The same types of condensate cloud particles are calculated to condense on Saturn, and there is no compelling reason to believe that the same types of particles should be more effective as catalysts on Saturn than on Jupiter. There is also no evidence for heterogeneous catalysis of PH_3 destruction on Saturn and not on Jupiter.

The (apparent) partitioning of He into Saturn's core may indicate similar behavior for ice- and rock-forming elements on Saturn. Thus, Saturn's atmosphere may be depleted in Ge instead of having a Ge abundance of 2.5 times solar as assumed in our calculations. Again, credible arguments suggest that this proposed mechanism is not significant for Ge. Both P and Ge are rock-forming elements which are expected to be accreted in their solar P/Ge ratio. Thus, if rock-forming elements were depleted by partitioning into Saturn's core, equal P and Ge depletions would be expected. The observation of PH_3 in Saturn's atmosphere shows that equal P and Ge depletions have not occurred. Selective Ge partitioning into Saturn's core cannot be unambiguously ruled out. However, Stevenson (1982) has argued that accretion of icy planetesimals after Saturn's formation has enriched the upper atmosphere in heavier constituents, which presumably includes rock constituents like Ge.

Another alternative is that the reported GeH_4 upper limit is not representative of its global tropospheric abundance on Saturn. This could be due to observational problems or to the fact that Saturn's 5 μm spectral window is not associated with "hot spots" in the planetary cloud cover, as is the case on Jupiter. Larson *et al.* (1980) report that Saturn's 5 μm brightness temperature (190 K, vs. 300 K for Jupiter) originates not

TABLE 1

PREDICTED AND OBSERVED MIXING RATIOS OF CHEMICAL PROBES ON JUPITER AND SATURN

	JUPITER[a]			SATURN[c]		
	Quench Temperature[a]	Mixing Ratio		Quench Temperature	Mixing Ratio	
PROBE	(K)	Predicted	Observed[b]	(K)	Predicted	Observed[d]
PH_3[e]	1240	5×10^{-7}	$6 \pm 2 \times 10^{7}$	1190	10^{-6}	$\sim 10^{-6}$
GeH_4[e]	900	6×10^{-10}	$7 \pm 2 \times 10^{-10}$	870	7×10^{-9}	$< 10^{-10}$
CO[f]	1070	$\leq 10^{-9}$	10^{-9}	860–970	$0.07–1.3 \times 10^{-10}$	?
N_2[g]	850–1600	$0.8–9 \times 10^{-6}$	?	870–1380	$0.2–2 \times 10^{-6}$	?

[a] Predictions assume solar composition and $K = 2 \times 10^8$ cm^2 s^{-1}.
[b] Observed mixing ratios from Larson, Fink, and Treffers 1978 and Kunde *et al.* 1982.
[c] Predictions assume 2.5 times solar composition and $K = 2 \times 10^8$ cm^2 s^{-1}.
[d] Observed mixing ratios from Larson *et al.* 1980.
[e] Predictions assume $k_{18} = k_{26} \approx 10^{-9}$ cm^3 s^{-1}.
[f] Jupiter values from Prinn and Barshay 1977.
[g] Jupiter values from Prinn and Olaguer 1981.

from deep in the atmosphere but from levels immediately above the visible cloud tops.

If the reported GeH_4 upper limit is valid, it may indicate that GeH_4 destruction occurs above the visible clouds on both Jupiter and Saturn by another irreversible process such as solar UV photolysis or reactions with H atoms from NH_3 or PH_3 photolysis. Mahncke and Noyes (1935) studied the UV absorption spectrum of GeH_4 and reported absorption coefficients for the 160–170 nm region. The absorption is apparently continuous, and the ultimate photochemical decomposition products are metallic Ge and H_2. Interestingly, the absorption cross section of GeH_4 is large in the wavelength region longward of the strong C_2H_6 and CH_4 absorptions at ≤ 160 nm but shortward of the strong C_2H_2, PH_3, and NH_3 absorptions above 170 nm.

A one-dimensional chemical-dynamical model was used to model GeH_4 photolysis in the 140–180 nm region at a latitude of 30° in Saturn's upper atmosphere. The solar UV flux digitized in 5 nm increments was obtained by scaling to Saturn the data of Heath and Thekaekara (1977). Absorption coefficients σ for CH_4, C_2H_6, C_2H_2, NH_3, PH_3, and GeH_4 were taken from Mount, Warden, and Moos (1977), Mount and Moos (1978), Strobel (1973), Sullivan and Holland (1966), Kley and Welge (1965), Halmann (1963), and Mahncke and Noyes (1935). The available GeH_4 absorption coefficients were extrapolated down to $\sigma = 7 \times 10^{-24}$ cm^2 at 180 nm and taken constant at $\sigma = 10^{-17}$ cm^2 at ≤ 160 nm. Vertical distribution profiles for CH_4, C_2H_2, C_2H_6, PH_3, and NH_3 were taken from Prinn *et al.* (1984). The PH_3 profile T1 was used above the 100 mbar level, and a constant PH_3 mixing ratio of 1×10^{-6} was assumed at lower levels. A GeH_4 mixing ratio of 7×10^{-9} at the lower boundary (1.7 bars) was used.

Calculations of t_{chem} for GeH_4 photolysis were done at 10 km increments in the 30–500 mbar region (which was also studied by Kaye and Strobel 1984). These photolysis lifetimes were computed ignoring the self-absorption by GeH_4, an assumption we justify *a posteriori*. The results show $t_{chem} = 5.7 \times 10^8$–$4.5 \times 10^{19}$ s in the 30–500 mbar region with most of the GeH_4 photolysis occurring in the upper 30 km of this region. These t_{chem} values are longer than the convective mixing times $t_{conv} = 4H^2/K$ calculated from the three vertical eddy diffusion coefficient profiles in the upper atmosphere model of Kaye and Strobel (1984). (Profile A represents slow vertical mixing, $K \approx 10^4$ cm^2 s^{-1}, near the NH_3 cloud level; profile B represents rapid vertical mixing, $K \approx 10^5$ cm^2 s^{-1}, up to just below the tropopause but decreasing to 10^4 cm^2 s^{-1} just above the tropopause; and profile C with $K = 10^5$ cm^2 s^{-1} independent of altitude.) Consequently, except in the upper 30 km of this region, photolysis is not an important loss mechanism for GeH_4. Hydrogen abstraction by reaction with H atoms,

$$H + GeH_4 \rightarrow GeH_3 + H_2 , \quad (29)$$

appears to be in comparison a much more important loss mechanism for GeH_4.

Austin and Lampe (1977) and Choo, Gaspur, and Wolf (1975) both reported values for k_{29} at 300 K. Unfortunately, these two determinations disagree by a factor of 215. We have therefore done calculations with both values by adopting the estimated activation energy (Austin and Lampe 1977) of 2.5 kcal mole^{-1} for SiH_4 abstraction for reaction (29) as well. The two derived expressions for k_{29} are denoted "fast" (Choo, Gaspur, and Wolf 1975) and "slow" (Austin and Lampe 1977):

$$\text{"fast"}\ k_{29} = 2.7 \times 10^{-8} \exp(-1258/T)\ \text{cm}^3\ \text{s}^{-1} , \quad (30)$$

$$\text{"slow"}\ k_{29} = 1.2 \times 10^{-10} \exp(-1258/T)\ \text{cm}^3\ \text{s}^{-1} . \quad (31)$$

Using these two values, together with the upper atmosphere model, vertical eddy diffusion coefficient profiles, and H atom concentration profiles of Kaye and Strobel (1984), we estimate the chemical lifetime of GeH_4 due to hydrogen abstraction in Saturn's upper atmosphere from $t_{chem} = 1/k_{29}[H]$.

The chemical lifetime of GeH_4 due to photolysis and hydrogen abstraction is plotted in Figure 7, where the "long" and "short" t_{chem} profiles correspond to the "slow" and "fast" expressions for k_{29}, and the t_{conv} profiles A, B, C refer to the three vertical eddy diffusion coefficient profiles of Kaye and Strobel (1984). Hydrogen abstraction is an efficient GeH_4 destruction mechanism in the 30–500 mbar region of Saturn's upper atmosphere if vertical mixing is relatively slow (profiles A and B) and if the "fast" expression for k_{29} is appropriate.

GeH_4 concentration profiles were calculated for the three t_{conv} profiles using the "short" t_{chem} values. Since GeH_4 is not an important source of H atoms, its profile can be derived simply from the formulae

$$f(z) = f(0) \exp[-z/h] , \quad (32)$$

$$h = [-1/2H + (1/4H^2 + 1/Kt_{chem})^{1/2}]^{-1} \quad (33)$$

(Prinn *et al.* 1984), where f is the mixing ratio of GeH_4, z is altitude, h is the mixing ratio scale height, and the GeH_4 mixing ratio is 7×10^{-9} at $z = 0$(1.7 bars). The t_{chem} and t_{conv} profiles in Figure 7 were extrapolated down to the 1.7 bar level in Saturn's atmosphere in these calculations. Figure 8 displays the resulting GeH_4 concentration profiles and shows that GeH_4 mixing ratios less than 10^{-10} are obtained in cases A and B but not C (where $K = 10^5$ cm^2 s^{-1} throughout the region considered). Self-absorption of UV by GeH_4 is negligible for each of the profiles shown. Essentially no dropoff in GeH_4 is obtained in cases A and C for the "long" t_{chem} profiles (Fig. 7), and the concentration profile for case B for the "long" t_{chem} is very similar to case C for the "short" t_{chem}. Note that, even in the unlikely case of no depletion, GeH_4 is not a dominant source of UV opacity. Thus, for relatively slow vertical mixing and the faster of two hydrogen abstraction rate constants, we conclude that substantial GeH_4 depletions can be produced several tens of kilometers above the NH_3 cloud base on Saturn (located at 1.7 bars, 162 K for 2.5 times solar composition; Prinn *et al.* 1984).

The final alternative which we have considered is that vertical mixing in Saturn's deep atmosphere is slower than on Jupiter. In this case, less GeH_4 would be transported into the upper atmosphere. The effects of varying eddy diffusion coefficients on the "quenched" abundances of PH_3 and GeH_4 are illustrated in Figure 6. The PH_3 abundance is independent of the assumed eddy diffusion coefficient until $K \approx 3 \times 10^6$ cm^2 s^{-1}; however, the GeH_4 abundance decreases with decreasing K over the entire range considered. An eddy diffusion coefficient of 5×10^2 cm^2 s^{-1} is large enough to provide the solar abundance of PH_3 in Saturn's upper atmosphere (consistent with the lower range of the PH_3 observations summarized by Prinn *et al.* 1984) but gives only 25% of the calculated GeH_4 abundance in our baseline model. This GeH_4 mixing ratio, 2×10^{-9}, is still 20 times larger than the reported GeH_4 upper limit; a GeH_4 mixing ratio of 2×10^{-10} consistent with the

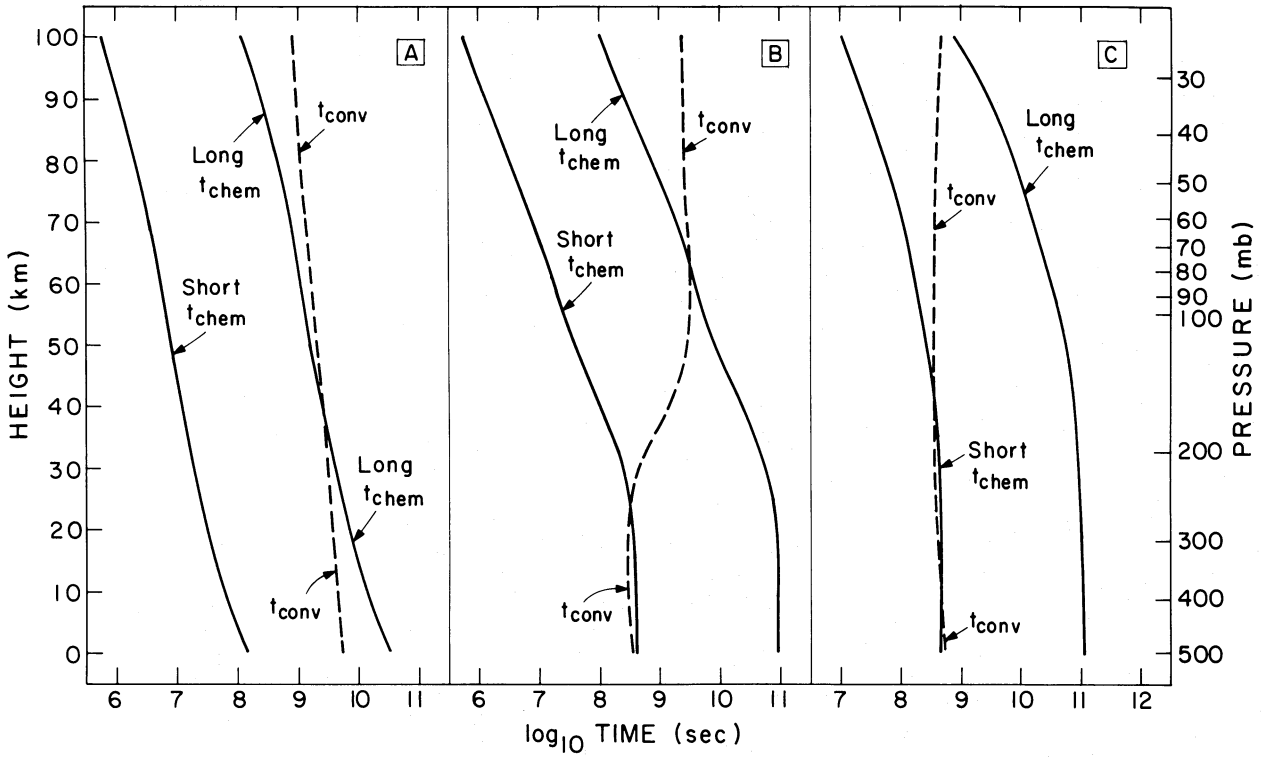

FIG. 7.—Comparison of GeH_4 chemical lifetime t_{chem} due to hydrogen abstraction and photo-dissociation with convective mixing times t_{conv} in Saturn's upper atmosphere. The three separate diagrams correspond to the three vertical eddy diffusion coefficient profiles in Kaye and Strobel (1984). The "long" and "short" t_{chem} profiles correspond to two different rate constants for hydrogen abstraction from GeH_4 (see text).

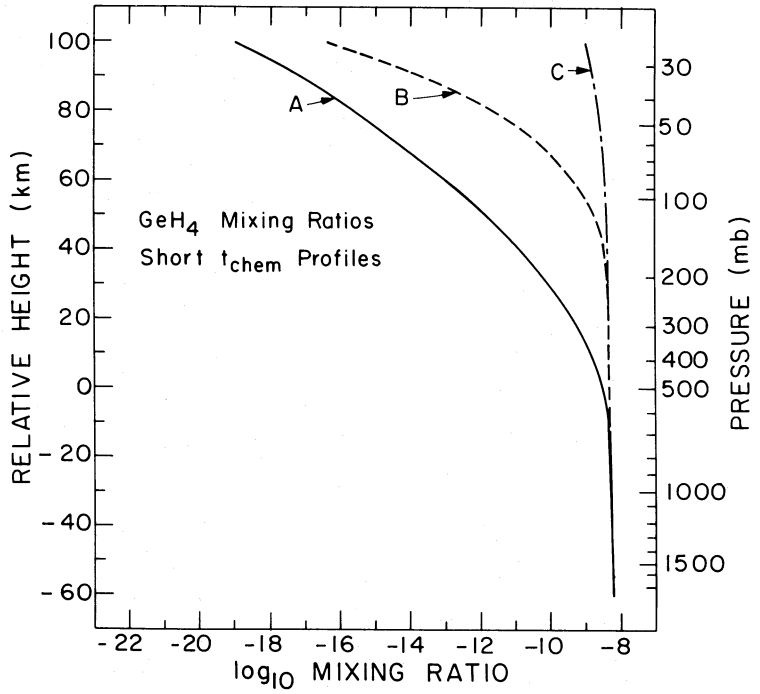

Fig. 8.—GeH_4 concentration profiles in Saturn's upper atmosphere. Three profiles corresponding to the "short" t_{chem} profiles for the three assumed vertical eddy diffusion coefficient profiles are shown. The "long" t_{chem} profiles yield essentially no GeH_4 depletion except for case B, which is very similar to curve C (see text).

upper limit requires $K = 1$ cm^2 s^{-1}. Values of K as low as 1–500 cm^2 s^{-1} are totally at odds with the values needed to explain transport of heat from the interior. Even if such values of K were possible, it is clear that we could not explain simultaneously the observed PH_3 and GeH_4 abundances using the same K value.

The abundances of two other potential chemical probes (CO and HCN) show large variations with changes in the assumed eddy diffusion coefficient and in principle are thus very useful for constraining vertical mixing rates. The calculated abundance profiles as a function of the assumed eddy diffusion coefficients are given in Figure 5 for CO, HCN, and N_2. The predicted CO mixing ratio corresponding to $K = 2 \times 10^8$ cm^2 s^{-1} in our baseline model is 1.3×10^{-10} for gas-phase destruction and 7×10^{-12} for iron-catalyzed destruction. A Jupiter-like CO mixing ratio of 10^{-9} would require $K > 2 \times 10^{10}$ cm^2 s^{-1}, which is very unlikely. No CO abundance estimates are available for Saturn, and in any case there is a plausible competing source for CO to that discussed in this paper. In particular, Prather, Logan, and McElroy (1978) and Strobel and Yung (1979) described models for CO production in Jupiter's upper atmosphere utilizing meteoritic debris and the Galilean satellites, respectively, as sources of extra-Jovian oxygen. It is certainly plausible that Saturn's rings may act as extra-Saturnian oxygen sources and that similar mechanisms to those proposed by Prather *et al.* and Strobel and Yung may operate on Saturn. Thus, spectroscopic observations of CO on Saturn (or Jupiter) cannot unambiguously be interpreted in terms of a vertical mixing source unless vertical distributions can be measured or inferred from the observations.

Observational upper limits (Larson *et al.* 1980; Tokunaga *et al.* 1981) are available for HCN on Saturn. The more stringent upper limits of Tokunaga *et al.* (1981) correspond to an HCN mixing ratio of 7×10^{-9} in Saturn's troposphere and 8×10^{-9} in Saturn's stratosphere. From Figure 5 we see that these upper limits correspond to $K < 4 \times 10^{14}$ cm^2 s^{-1}. This is not a useful upper bound to the eddy diffusion coefficient in Saturn's deep atmosphere, since the eddy vertical transport velocity is certainly constrained to be less than the sound speed v_s (~ 3.0–4.3×10^5 cm s^{-1} in the 1000–2000 K region), so the eddy diffusion coefficient is certainly constrained by

$$K < v_s H \approx 1\text{–}3 \times 10^{13} \text{ cm}^2 \text{ s}^{-1} , \quad (34)$$

where v_s is calculated for a solar composition H_2 + He gas. Using expression (34), the maximum HCN abundance which can be provided by vertical mixing corresponds to a mixing ratio of $\sim 5 \times 10^{-9}$, which is already 20%–80% smaller than the spectroscopic upper limits.

Kaye and Strobel (1984) predicted HCN abundances produced by solar UV photolysis in Saturn's upper atmosphere. Their predictions yield HCN mixing ratios less than 10^{-12} at the 500 mbar level in Saturn's atmosphere, depending on their assumed eddy diffusion coefficient profiles. These mixing ratios are comparable to HCN mixing ratios predicted for vertical mixing with $K < 3 \times 10^1$ cm^2 s^{-1} and are over 100 times smaller than the predicted HCN mixing ratio of 2×10^{-10} in our baseline model (in which $K = 2 \times 10^8$ cm^2 s^{-1}). Therefore, it appears that vertical mixing may dominate over photochemistry as a source of HCN in Saturn's troposphere. Assuming that HCN and CH_3NH_2 remain in conditional chemical equilibrium with each other, vertical mixing will supply more CH_3NH_2 than HCN by several orders of magnitude (see Fig. 2). Kaye and Strobel (1984) also included CH_3NH_2 in their calculations and found calculated column densities $\sim 10^2$–10^3 times smaller than their calculated HCN column densities. Thus, it also appears that vertical mixing may dominate photochemistry as a source of tropospheric CH_3NH_2.

Atreya, Kuhn, and Donahue (1980) predicted N_2 mixing ratios in Saturn's upper atmosphere by considering solar UV photolysis of NH_3. They calculated N_2 mixing ratios of 1.8×10^{-10} to 6×10^{-8} (depending on the amount of NH_3 and N_2H_4 supersaturation) at the visible cloud tops. By contrast, the predicted N_2 mixing ratios in our baseline model (which has 2.5 times solar NH_3) are in the range $0.2\text{–}2 \times 10^{-6}$ depending on whether heterogeneous catalysis is effective. The homogeneous gas-phase reactions which we have considered for N_2 do not yield mixing ratios less than 10^{-6} for all K values considered (Fig. 5). The heterogeneous iron-catalyzed reactions do yield lower N_2 mixing ratios, but eddy diffusion coefficients greater than 10^{13} cm^2 s^{-1} are required to get N_2 mixing ratios as low as those produced photochemically (for reasonable Fe particle sizes which could be transported into the upper atmosphere). Therefore, we also conclude that the dominant source of N_2 in Saturn's troposphere (as on Jupiter) is vertical mixing.

Finally, we have also considered possible chemical probes of other elements by scaling the calculations of Barshay and Lewis (1978) and Fegley and Lewis (1979) to Saturn. This exercise suggests that very few additional chemical probes with potentially observable abundances are expected on Saturn. The "short list" of probes and their maximum predicted mixing ratios (for our 2.5 times solar composition baseline model) are as follows: H_2Se ($\sim 10^{-8}$), AsH_3 ($\sim 10^{-9}$), InBr ($\sim 10^{-10.5}$), Tl ($\sim 10^{-10.5}$), and SbS ($\sim 10^{-10.3}$).

VI. CONSTRAINTS ON THE COMPOSITION OF SATURN'S ATMOSPHERE

The relative abundances of some chemical probes such as PH_3, CO, and N_2 are also potentially useful for constraining the composition of Saturn's bulk atmosphere. Current models for the formation of Saturn lead to the prediction that Saturn's bulk composition is enriched in ice- and rock-forming elements to varying amounts (see, e.g., Stevenson 1982). The available spectroscopic data reviewed by Prinn *et al.* (1984) also show that Saturn's upper atmosphere is enriched in CH_4, NH_3, and PH_3 by factors of 2.5, 1–3, and 1–4 times, respectively, relative to the solar composition values. Thus it is worthwhile considering cases where ice- and rock-forming elements such as C, N, O, P, and Ge are enriched by factors greater than 2.5 relative to solar composition. As shown by Prinn *et al.* (1984), this is easily accomplished by examination of the equilibria involved to define scaling laws which relate the enriched cases to our baseline case. If the enrichment factor for elements heavier than H and He relative to our baseline model is E, and the enrichments are not so large as to influence the mixing ratios of H_2 and He, then the equilibrium CO and N_2 mixing ratios both simply increase by a factor of E^2. According to equations (7) and (8) the CO and N_2 chemical lifetimes are independent of E, so the CO and N_2 mixing ratios predicted for a given K value also increase simply by a factor of E^2. Because the assumed net reaction (22) for GeH_4 destruction involves equimolar amounts of GeH_4 and H_2S, increases in the assumed elemental abundances do not alter the calculated GeH_4 abundance profile (Fig. 4). According to equation (27), the chemical lifetime of GeH_4 varies as E^{-1}, which produces a

decrease in the GeH_4 mixing ratio predicted for a given K value (Fig. 6), but the effect is relatively small. By contrast, the equilibrium PH_3 mixing ratios for $E > 1$ increase as E below the P_4O_6 condensation level and decrease as $E^{-5/4}$ above this level despite the increased P abundance. In addition, according to equation (21) the PH_3 chemical lifetime varies as E^{-1}, which leads to a further decrease in the PH_3 mixing ratio predicted for a given K value. The results for $E = 4$ and 20 for PH_3 are shown in Figure 6. For $E = 4$, eddy diffusion coefficients less than $\sim 10^7$ cm^2 s^{-1} yield less PH_3 by vertical mixing than in the baseline model. The situation is even more extreme in the $E = 20$ case, where all values of $K < 10^{10}$ cm^2 s^{-1} yield less PH_3 than in the baseline model. In fact, the latter model for the composition of Saturn's atmosphere is inconsistent with the observed PH_3 abundance range in Saturn's atmosphere except for very rapid vertical mixing ($K > 10^{10}$ cm^2 s^{-1}). Mixing rates this rapid in the $E = 20$ case would also yield CO and N_2 mixing ratios greater than $10^{-6.6}$ and $10^{-3.2}$ respectively.

VII. CONCLUDING REMARKS

The results of our thermochemical equilibrium and kinetic calculations show that the most abundant nonequilibrium species mixed up from Saturn's deep atmosphere are predicted to be N_2, PH_3, GeH_4, and CO. Other less abundant nonequilibrium species produced in the same way are HCN and CH_3NH_2. Vertical mixing appears to be the dominant source of all these species (except perhaps CO) in Saturn's troposphere. Because the abundances of these nonequilibrium species in the upper atmosphere depend on the thermochemistry and dynamics of the very deep atmosphere, they can be regarded as "chemical probes" of these deep, otherwise inaccessible, levels within the planet.

Three chemical probes, PH_3, CO, and GeH_4, have been observed on Jupiter, and our thermochemical kinetic calculations for PH_3 and GeH_4 satisfactorily account for their observed abundances on that planet. However, only PH_3 has been observed on Saturn, and the GeH_4 abundance is reported to be less than 10^{-10} (mixing ratio). The apparent paradox on Saturn is that the predicted GeH_4 abundance is 70 times larger than this reported upper limit. To resolve this paradox, we have shown that destruction of GeH_4 by reaction with H atoms (from NH_3 and PH_3 photodissociation) and by photodissociation is sufficiently rapid to deplete this gas at least above the tropopause on both Jupiter and Saturn. We propose that this depletion, combined with the fact that the spectroscopic observations at 5 μm on Saturn apply to much higher levels in the atmosphere than on Jupiter, is a possible reason why GeH_4 has not yet been observed at Saturn.

Although Courtin *et al.* (1984) and Fink *et al.* (1983) reported that the 5 μm flux is from the 170–190 K, 2 bars level, both groups also found NH_3 mixing ratios less than solar. This is in apparent conflict with the microwave data of Klein *et al.* (1978) indicating NH_3 mixing ratios of solar or greater beneath the NH_3 cloud base (153 K, 1.4 bars for solar NH_3, 162 K, 1.7 bars for 2.5 times solar NH_3). Thus, as Fink *et al.* (1983) conclude, the penetration depth of Saturn's 5 μm flux is still unclear.

It is possible to deduce vertical mixing rates in Saturn's deep atmosphere by using the above chemical probes. Our calculations show that CO, GeH_4, and HCN are most useful for this purpose, while N_2 has a relatively flat abundance profile versus assumed eddy diffusion coefficients and is less sensitive in this regard. At the moment a vertical eddy diffusion coefficient $K > 10^6$ cm^2 s^{-1} appears adequate to explain the PH_3 levels on Saturn. Observations of (any of) the other chemical probes mentioned above will be required to constrain the K value better.

Note added in manuscript 1985 July 31.—Noll, Knacke, and Tokunaga (Goddard Institute for Space Studies Conf. on Outer Planets, 1985 May) reported the detection of CO on Saturn at a mixing ratio of $3 \pm 2 \times 10^{-9}$. This abundance implies unrealistically rapid vertical mixing ($K \approx 2.5 \times 10^{11}$ cm^2 s^{-1}) if the CO is solely due to rapid vertical mixing. If the CO mixing ratio is indeed this large, then the major source must be CO production in Saturn's upper atmosphere.

This work was supported by NSF grant ATM-84-01232 to MIT.

REFERENCES

Atreya, S. K., Kuhn, W. R., and Donahue, T. M. 1980, *Geophys. Res. Letters*, **7**, 474.
Atreya, S. K., and Romani, P. N. 1985, in *Planetary Meteorology*, ed. G. E. Hunt (Cambridge: Cambridge University Press), p. 17.
Austin, E. R., and Lampe, F. W. 1977, *J. Phys. Chem.*, **81**, 1134.
Barshay, S. S., and Lewis, J. S. 1978, *Icarus*, **33**, 593.
Beer, R., and Taylor, F. W. 1978, *Ap. J.*, **221**, 1100.
Cameron, A. G. W. 1982, in *Essays in Nuclear Astrophysics*, ed. C. A. Barnes, D. D. Clayton, and D. N. Schramm (Cambridge: Cambridge University Press), p. 23.
Choo, K. Y., Gaspur, P. P., and Wolf, A. P. 1975, *J. Phys. Chem.*, **79**, 1752.
Courtin, T., Gautier, D., Marten, A., Bezard, B., and Hanel, R. 1984, *Ap. J.*, **287**, 899.
Fegley, B., Jr., and Lewis, J. S. 1979, *Icarus*, **38**, 166.
Fink, U., and Larson, H. P. 1978, *Science*, **201**, 343.
Fink, U., Larson, H. P., Bjoraker, G. L., and Johnson, J. R. 1983, *Ap. J.*, **268**, 880.
Fink, U., Larson, H. P., and Treffers, R. R. 1978, *Icarus*, **34**, 344.
Flasar, M., and Gierasch, P. 1977, in *Proceedings: Symposium on Planetary Atmospheres*, ed. A. Vallance-Jones (Ottawa: Royal Society of Canada), p. 85.
Glushko, V. P., Gurvich, L. V., Bergman, G. A., Veitz, I. V., Medvedev, V. A., Khachkuruzov, G. A., and Yungman, V. S. 1978–1982, ed., *Thermodynamic Properties of Individual Substances*, 4 vols. (Moscow: High-Temperature Institute).
Halmann, M. 1963, *J. Chem. Soc.* (London), p. 2853.
Hanel, R., *et al.* 1981, *Science*, **212**, 192.
Heath, D. F., and Thekaekara, M. P. 1977, in *The Solar Output and its Variation*, ed. O. R. White (Boulder: Associated Universities Press), p. 193.
Hubbard, W. B., and Stevenson, D. J. 1984, in *Saturn*, ed. T. Gehrels and M. S. Matthews (Tucson: University of Arizona Press), p. 47.
Kaye, J. A., and Strobel, D. F. 1984, *Icarus* **59**, 314.
Kelley, K. K. 1960, *Contributions to the Data on Theoretical Metallurgy*, Vol. **13**, *High-Temperature Heat-Content, Heat-Capacity, and Entropy Data for the Elements and Inorganic Compounds* (Washington: US Bureau of Mines, Bull. No. 584).
Kelley, K. K., and King, E. G. 1961, *Contributions to the Data on Theoretical Metallurgy*, Vol. **14**, *Entropies of the Elements and Inorganic Compounds* (Washington: US Bureau of Mines, Bull. No. 592).
Klein, M. J., Janssen, M. A., Gulkis, S., and Olsen, E. T. 1978, in *The Saturn System*, ed. D. M. Hunten and D. Morrison (NASA Conf. Pub. 2068), p. 195.
Kley, D., and Welge, K. H. 1965, *Zs. Naturforschung*, **20A**, 124.
Kunde, V., *et al.* 1982, *Ap. J.*, **263**, 443.
Larson, H. P., Fink, U., Smith, H. A., and Davis, D. S. 1980, *Ap. J.*, **240**, 327.
Larson, H. P., Fink, U., and Treffers, R. R. 1978, *Ap. J.*, **219**, 1084.
Larson, H. P., Treffers, R. R., and Fink, U. 1977, *Ap. J.*, **211**, 972.
Lewis, J. S., 1969, *Icarus*, **10**, 393.
Lewis, J. S., and Fegley, B., Jr. 1984, *Space Sci. Rev.*, **39**, 163.
Mahncke, H. E., and Noyes, W. A., Jr. 1935, *J. Am. Chem. Soc.*, **57**, 456.
Mount, G. H., and Moos, H. W. 1978, *Ap. J.*, **224**, L35.
Mount, G. H., Warden, E. S., and Moos, H. W. 1977, *Ap. J.*, **214**, L47.
Prather, M. J., Logan, J. A., and McElroy, M. B. 1978, *Ap. J.*, **223**, 1072.
Prinn, R. G., and Barshay, S. S. 1977, *Science*, **198**, 1031.
Prinn, R. G., and Fegley, B., Jr. 1981, *Ap. J.*, **249**, 308.

Prinn, R. G., Larson, H. P., Caldwell, J. J., and Gautier, D. 1984, in *Saturn*, ed. T. Gehrels and M. S. Matthews (Tucson: University of Arizona Press), p. 88.
Prinn, R. G., and Olaguer, E. P. 1981, *J. Geophys. Res.*, **86**, 9895.
Ridgway, S. T., Larson, H. P., and Fink, U. 1976, in *Jupiter*, ed. T. Gehrels (Tucson: University of Arizona Press), p. 348.
Stevenson, D. J. 1982, *Planet. Space Sci.*, **30**, 755.
Stone, P. H. 1976, in *Jupiter*, ed. T. Gehrels (Tucson: University of Arizona Press), p. 586.
Strobel, D. F. 1973, *J. Atmos. Sci.*, **30**, 489.
Strobel, D. F., and Yung, Y. L. 1979, *Icarus*, **37**, 256.
Stull, D. R., and Prophet, H. 1971–1985, *JANAF Thermochemical Tables* (2d ed. and subsequent supplements; Washington: NBS).
Stull, D. R., Westrum, E. F., Jr., and Sinke, G. C. 1969, *The Chemical Thermodynamics of Organic Compounds* (New York: Wiley).
Sullivan, J. O., and Holland, A. C. 1966, NASA Contract Rept. 371.
Tokunaga, A. T., Beck, S. C., Geballe, T. R., Lacy, J. H., and Serabyn, E. 1981, *Icarus*, **48**, 283.
Wagman, D. D., Evans, W. H., Parker, V. B., Halow, I., Bailey, S. M., and Schumm, R. H. 1968, *Selected Values of Chemical Thermodynamic Properties: Tables for the First Thirty-Four Elements in the Standard Order of Arrangement* (NBS Tech. Note, No. 270–3).
Weidenschilling, S. J., and Lewis, J. S. 1973, *Icarus*, **20**, 465.

BRUCE FEGLEY, JR., and RONALD G. PRINN: Dept. of Earth, Atmospheric and Planetary Sciences, Massachusetts Institute of Technology, Cambridge, MA 02139